Structural Behaviour of Ferrocement channels Beams

Yousry B.I. Shaheen[(1)], Noha M. Soliman[(2)], Ashwaq M. Hafiz[(3)]

[(1)]*Professor of Strength and Testing of Materials, Faculty of Engineering, Menoufia University, EGYPT.*

[(2)]*Lecturer at Department of Civil Engineering, Faculty of Engineering, Menoufia University, EGYPT.*

[(3)]*Graduate student, Civil Engineering Department, Menoufia University, EGYPT*

Abstract

The main objective of this research is to study the structural behaviour of ferrocement concrete composite channels reinforced with various types of reinforcing materials. The dimensions of the developed ferrocement and control test specimens were kept constant as 100 mm width, 200 mm height and 2000 mm length. The thickness of the two webs and base was kept constant as 25 mm. The test specimens were loaded under four point loadings until failure. The effects of the main parameters were extensively studied. High resistance ferrocement channels beams were developed with high crack resistance, high deformation characteristics, high strength, high ductility and energy absorption properties could be used with great economic advantages in the same way as steel channels in some of its uses and very useful for developed and developing countries alike.

Keywords: Ferrocement channels; Deformation characteristics; Strength; Serviceability load; Cracking behaviour; Ductility; Energy absorption.

1.   Introduction

Recently, ferrocement has emerged as new construction material. ACI committee 549 [1] defines ferrocement as follows: "Ferrocement is a type of reinforced concrete commonly constructed of hydraulic cement mortar reinforced with closely spaced layers of relatively small wire diameter mesh. The mesh may be made of metallic or other suitable materials. The fineness of the mortar matrix and its composition should be compatible with the opening and tightness of the reinforcing system it is meant to encapsulate. The matrix may contain discontinuous fibres [2, 3].

1945 Nervi built the first ferrocement structure then a vaulted roof over shopping centre was built in Leningrad in Soviet Union In 1974. In 1975, two ferrocement aqueducts were designed & built for rural irrigation in China [4]. Ferrocement is now recognized as a construction material with excellent qualities of crack control, impact resistance, and toughness, largely due to the close spacing and uniform dispersion of reinforcement within the material. Many investigations have clarified the physical and mechanical properties of this material, and numerous test data are available to define its performance criteria for design and construction [(5-9)].

Structural Applications of Ferrocement were Boats, Tanks, Silos, Roofs, Repair and Strengthening of Structures. The successful usage of ferrocement in repairing and construction of reinforced concrete beams and the high cost of traditional wooden or steel form work led to the idea of using ferrocement laminate as permanent forms in concrete construction. [10-24]

Abdul Kadir and Jaafar (1993) [12, 21, 22] offered a proposed technique for using ferrocement concept to produce in situ permanent formwork as a viable alternative of traditionally used wooden forms. Then Mays and Barnes (1995) [19] studied the feasibility of using precast ferrocement as a low permeability cover layer to the subsequently poured in situ reinforced concrete members located in environments, where there is a high risk of reinforcement corrosion. The research focused particularly on achieving an adequate and durable bond between the ferrocement layer and the concrete core in order to develop composite structural behaviour. The use of permanent ferrocement formwork provided an increase in strength of 15% over the conventional reinforced concrete.

Abdul Kadir et al. (1997) [13] presented the results of test on the flexural behaviour of reinforced concrete beams with ferrocement permanent formwork. The beams incorporating ferrocement formwork contributed from 16 to 75% to the flexural strength of the composite beams depending on steel area and the use of shear connectors. The ferrocement forms incorporating reinforced concrete core with shear connectors achieved higher strength by an average of 10% compared to the ones without shear connectors; however, they showed lower deflections when subjected to the same load.

Abdel Tawab (2006) [11] presented the results of an investigation aiming at the development of U-shaped ferrocement permanent forms to be used for construction of reinforced concrete beams as a viable alternative to traditionally used wooden and metal formwork. Ashwaq M. Hafiz (2012) [25] studied the behaviour of ferrocement concrete composite channels reinforced with various types of reinforcing materials under failure load. The results showed that high ultimate and serviceability loads, crack resistance control, high ductility, and good energy absorption properties could be achieved by using the proposed permanent ferrocement forms. Many of researchers studied the application of ferrocement in structural buildings [1, 11-13, 19, 26].

2.   Experimental program

The experimental program held in this study was performed in the laboratory of testing of building materials at the Faculty of Engineering, Menoufia University, Egypt. The experimental program was divided into two phases, the first phase regarding the reinforcement, in this program, fourteen specimens were cast and tested in order to study their behaviour under flexural loadings (see Table 1).There are designed according to Egyptian code of practice (E.C.P. 203/2007) [27].

The main objective was to determine the mechanical properties of the used steel and wire meshes. The second phase, the main objective was studying the ultimate load, flexural behaviour, ductility ratio, energy absorption and mode of failure at collapse of the control beams, which were reinforced with steel and to compare their behaviour with those conventional reinforced ferrocement beams reinforced with expanded metal mesh, welded metal mesh and glass fibre mesh.

2.1. Materials

1) **The fine aggregate** used in the experimental program was of natural siliceous sand. Its characteristics satisfy the (E.C.P. 203/2007) [27], (E.S.S. 1109/2008) [28]. It was clean and nearly free from impurities with a specific gravity 2.6 t/m^3 and a modulus of fineness 2.7.

2) **The cement** used was the Ordinary Portland cement, type produced by the Suez cement factory. Its chemical and physical characteristics satisfied the Egyptian Standard Specification (E.S.S. 4657-1/2009) [29].

3) **The water** used was the clean drinking fresh water free from impurities used for mixing and curing the R.C. beams tested according to the (E.C.P. 203/2007) [27].

4) **Super plasticizer** used was a high rang water reducer HRWR. It was used to improve the workability of the mix. The admixture used was produced by CMB GROUP under the commercial name of Addicrete BVF. It meets the requirements of ASTM C494 (type A and F) [30]. The admixture is a brown liquid having a density of 1.18 kg/litre at room temperature. The amount of HRWR was 1.0 % of the cement weight.

5) **Reinforcing Steel:** Normal mild steel bars were used, produced from the Ezz Al Dekhila Steel - Alexandria Its chemical and physical characteristics satisfy the Egyptian Standard Specification (E.S.S. 262/2011) [31]. Mild steel bars of 6 mm diameter were used for stirrups with yield strength of 240 MPa.

6) **Reinforcing Meshes**

a) **Expanded Metal Mesh:** Expanded metal mesh was used as reinforcement for ferrocement channels. The technical specifications and mechanical properties of expanded metal mesh as provided by producing company are given in Table 2. Figure 1 illustrates the photo of the expanded metal mesh.

b) **Welded Metal Mesh:** Galvanized welded metal mesh used was obtained from China. Welded metal mesh was used as reinforcement for ferrocement channels. The technical specifications and mechanical properties of welded metal mesh as provided by producing company are given in Table 2. Figure 1 illustrates the image.

c) **Fibreglass Mesh:** Fibreglass mesh used was obtained from Gavazzi Company, Italy, It was available in the Egyptian markets, the technical specifications and mechanical properties of Fibreglass mesh. The technical specifications and mechanical properties of Fibreglass mesh as provided by producing company are given in Table 2. Figure 1 illustrates the image.

7) **Polypropylene fibres PP 300-e3** was used. It was available in the Egyptian markets. It was used in concrete mixes to produced fibrous concrete jacket to improve the concrete characteristics. The percentage of addition was chosen as 900 gm/m^3 based on the recommendations of manufacture. The technical specifications and mechanical properties of Polypropylene fibres PP 300-e3 as provided by producing company are given in Table 3. Figure 1 illustrates the image.

2.2. Mortar Matrix

The concrete mortar used for casting channels was designed to get an ultimate compressive strength at 28-days age of (350 kg/cm^2), 35 MPa. The mix properties for mortar matrix were chosen based on the (ACI committee 549 report: 1988 [1]). For all mixes, mechanical mixer in the laboratory used mechanical mixing with capacity of 0.05 m^3, where the volume of the mixed materials was found to be within this range.

The constituent materials were first dry mixed; the mix water was added and the whole patch was re-mixed again in the mixer. The mechanical compaction was applied for all specimens. Mix properties by weight for the different groups are given below in Table 4. Figure 1 emphasizes the types of meshes used. Figure 2 shows reinforcement details and photos of all control and ferrocement channels.

2.3. Volume Fraction of Reinforcement (V_r%)

Volume Fraction of Reinforcement is the total volume of reinforcement per unit volume of ferrocement. For a composite reinforced with meshes with square openings, (V_r) is equally divided into (V_{rt}) and (V_{ri}) for the longitudinal and transverse directions, respectively[25,26].

TABLE1: DETAILS OF EXPERIMENTAL PROGRAM

Series designation	Beam No.	Volume fraction of reinforcement, %	Reinforcement details			
			Tension Steel bars, Ø 6 mm	Compression steel bars, Ø 6 mm	No. of stirrups, Ø 6 mm	No. And type of mesh layers
A	A1	2.314	3	2	12	----
	A2	2.407	3	2	12	------
B	B3	0.753	--	--	--	1 layer Expanded steel mesh
	B4	1.51	--	--	--	2 layers Expanded steel mesh
	B5	0.753	2	2	--	1layer Expanded steel mesh
	B6	1.51	2	2	--	2layers Expanded steel
C	C7	0.54	2	--	--	2 layers welded steel mesh
	C8	1.07	2	2	--	4 layers welded steel mesh
	C9	0.54	2	3	--	2 layers welded steel mesh
	C10	1.07	2	2	--	4 layers welded steel mesh
	C11	.0.54	2	2	--	2 layers welded steel mesh
	C12	1.07	3	2	---	4 layers welded steel mesh
D	D13	0.535	3	2	12	1 layer fibreglass steel mesh
	D14	1.07	3	2	12	2 layers fibreglass steel mesh

TABLE (2) TECHNICAL SPECIFICATIONS AND MECHANICAL PROPERTIES OF EXPANDED METAL MESH AND WELDED METAL MESH

Expanded Metal Mesh		Welded Metal Mesh		Fibreglass mesh		
Style	1532	Dimensions Size	12.5 × 12.5 mm	Dimensions Size	12.5 × 11.5 mm	
Sheet Size	1 m × 10	Weight	430 gm /m^2	Dimensions of strings	Longitudinal	1.66 *0.66 mm
Weight	1.3 Kg/m^2	Proof Stress	(N/mm^2) 400		Transverse	1* 0.5 mm
Diamond size	16 × 31mm	Ultimate Strength (N/mm^2)	600	Weight	123 g/m^2	
Dimensions of strand	1.25 × 1.5mm	Ultimate Strain × 10^{-3}	58.8	Volume fraction	0.535 %	
Proof Stress (N/mm^2)	199	Proof Strain × 10^{-3}	1.17	Tensile Strength	325 N/mm^2	
Proof Strain × 10^{-3}	9.7			Elongation	5.5 %	
Ultimate Strength (N/mm^2)	320					
Ultimate Strain× 10^{-3}	59.2					

TABLE (3) PHYSICAL AND MECHANICAL PROPERTIES OF POLYPROPYLENE FIBERS 300-E[3]

Fiber Length	Type / Shape	Absorption	Specific Gravity	Electrical Conductivity	Acid &Salt Resistance	Melt Point	Ignition Point	Thermal Conductivity	Alkali Resistance
Various	Graded / Fibrillated	Nil	0.91	Low	High	ºC(324º) 162	593 ºC(1100ºF)	Low	Alkali Proof

TABLE (4) FERROCEMENT MORTAR MIX PROPERTIES BY WEIGTHT /M3

Mix Design	Cement (kg/m^3)	Sand (kg/m^3)	Water (kg/m^3)	Super plasticizer (kg/m^3)	Fiber (kg/m^3)
M 1	681.82	1363.64	238.64	6.82	0.9
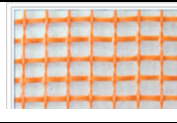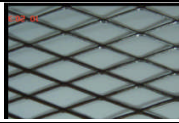
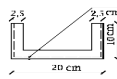| Expanded Metal Mesh	Welded Metal Mesh	Fiberglass Mesh	Polypropylene Fibers 300-e^3

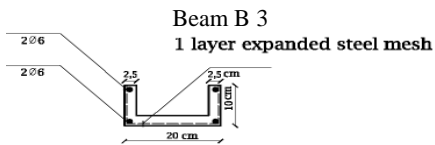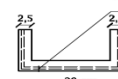**Figure 1. The Types of Meshes used and Polypropylene Fibers 300-e^3**
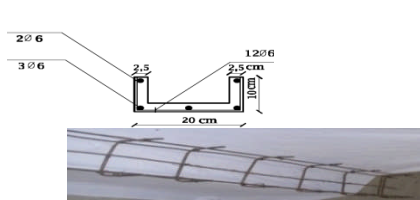
Beam A1
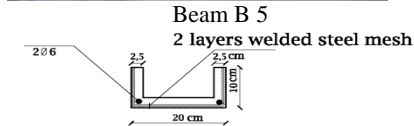1 layer expanded steel mesh
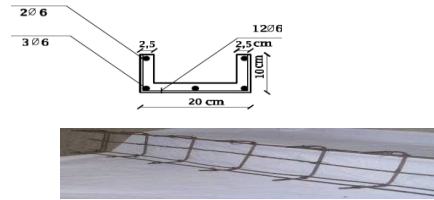
Beam A2
2 layers expanded steel mesh

Beam B 3
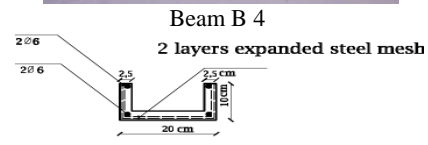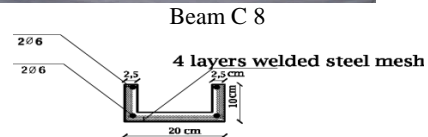
Beam B 4

Beam B 5
1 layer expanded steel mesh
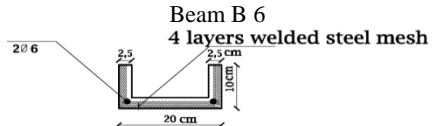
Beam B 6
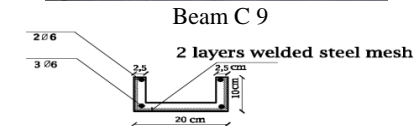2 layers expanded steel mesh
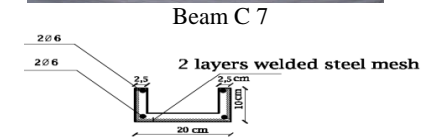
Beam C 7
2 layers welded steel mesh

Beam C 8
4 layers welded steel mesh

Beam C 9
2 layers welded steel mesh
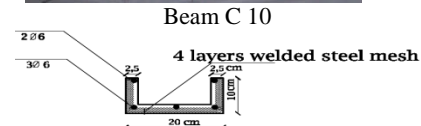
Beam C 10
4 layers welded steel mesh

Beam C 11
2 layers welded steel mesh

Beam C 12
4 layers welded steel mesh

Beam D 13
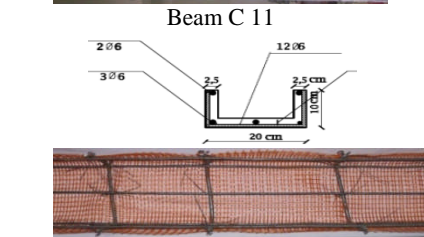
Beam D 14
2 layers fiberglass mesh
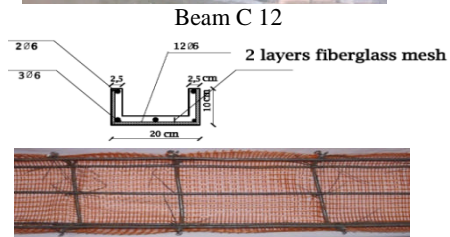
Figure 2. Reinforcement details of all beams

2.4.   Preparation of Test Specimens

A special wooden mold, Figure 3 was designed and manufactured to cast U-shaped ferrocement forms .The ferrocement U-shaped forms were prepared in the following sequence:

1. The wooden mold was assembled and the reinforcing steel mesh was formed in a U-shaped form and the steel bars of 6 mm diameter were tight with steel mesh inside the ferrocement U-shaped forms and placed in the vent of the mold. The constituents of the mortar were mixed and cast in each vent to the required thickness of 25 mm.

2. Wooden pans were placed on top of the cast ferrocement layer and the sides of the ferrocement forms were cast around the wooden pans in the vent of the wooden mold.

3. The ferrocement forms were left for 24 hours in the mold before disassembling the mold. At the end of this step, three U-shaped ferrocement forms are produced. The forms were covered with wet burlap for 28 days.
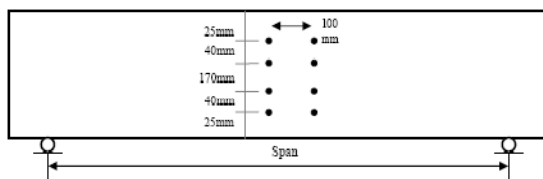

Figure 3. U shape Wooden Mold

Figure 4. Locations of Demec Sets   **Figure 5. Test Set up**

2.5.   Test Setup

At the time of testing, the specimen was painted with white paint to facilitate the visual crack detection during testing process. A set of eight demec points was placed on one side of the specimen to allow measuring the strain versus load during the test. Demec points were placed as shown in Figure 4.

The specimen was laid on a universal testing machine of maximum capacity of 100 kN where the test was conducted under a four-point loads system with a span of 1800 mm. Three dial gauges with an accuracy of 0.01 mm were placed under the test specimen at the centre to measure the deflection versus load. Load was applied at 5 kN increments on the specimen exactly at the centre. The horizontal distance between each pair of demec points was recorded by using a mechanical strain gauge reader. Concurrently, the beam deflections were determined by recording the dial gauge reading at each load increment. Cracks were traced throughout the sides of the specimen and then marked with red and black markers. The first crack-load of each specimen was recorded. The load was increased until complete failure of the specimen was reached. Figure 5 shows test set up.

3.   Experimental Results and Discussions

The experimental results of the test program and the discussions are presented. Comparisons are conducted between the results of the different test groups to examine the effect of the test parameters under investigation; existence of the permanent ferrocement forms, type of mesh

reinforcement. The effects of these parameters on the structural responses of the proposed beams in terms of failure load, mode of failure, first crack load, service load, ductility ratio, and energy absorption were studied extensively.

3.1 Flexural Serviceability Load

The Flexural serviceability load was calculated from the load-deflection curves. It is defined as the load corresponding to deflection equal to the span of the beam (1800 mm) divided by (constant = 250) according to The Egyptian Code (E.C.P. 203/2007) [7].

Figure 6 represents the values for the first cracking loads, serviceability loads and ultimate loads for all the tested beams. Maximum ultimate load reached for beam C12, while minimum ultimate load reached for beam B3.
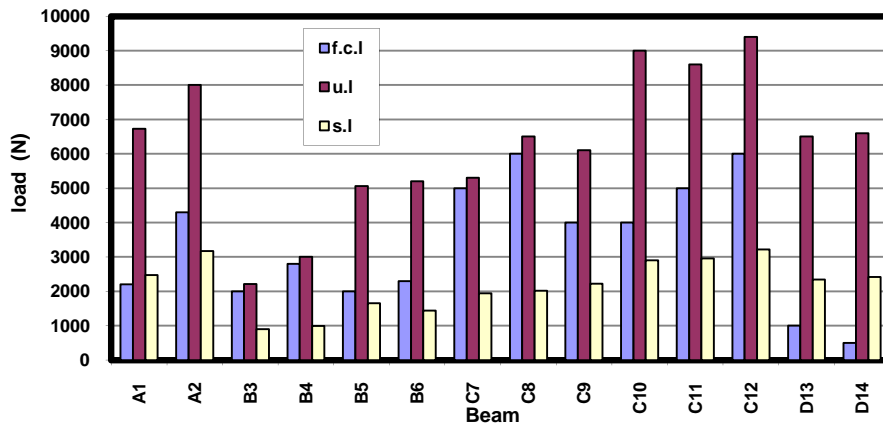

Figure 6. First crack loads, serviceability loads, and ultimate loads.

3.2 Ductility Ratio

The ductility ratio was calculated as ratio of the mid span deflection at the ultimate load to that at the first cracking load. Beams reinforced with expanded metal mesh and fibreglass mesh were given higher ductility ratio than control beam. Beams reinforced with welded metal mesh were given lower ductility ratio than control beam. Beams reinforced with welded metal mesh were given lower ductility ratio than beams reinforced with expanded metal mesh or fibreglass mesh, Figure 7.
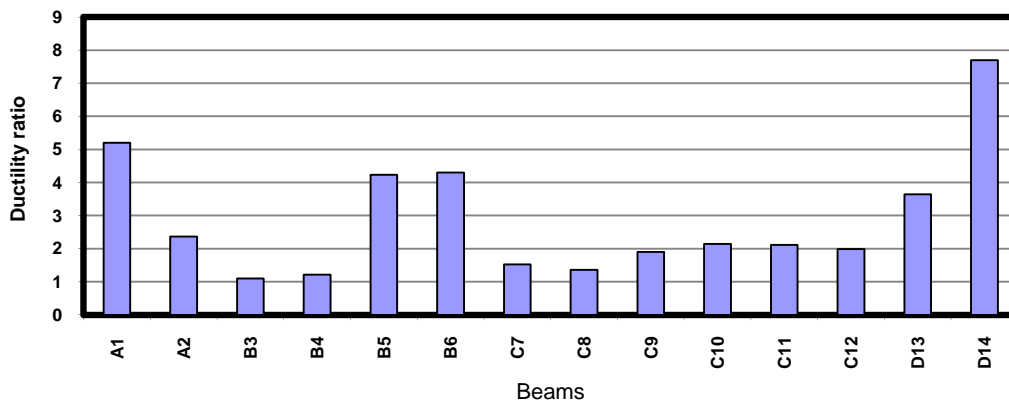

Figure 7. The ductility ratio for all beams.

3.3 Energy Absorption

The energy absorption was obtained by calculating the area under the load-deflection curve for each beam. Beams reinforced with expanded metal mesh were given lower energy absorption than control beam. Beams reinforced with welded metal mesh were given higher energy absorption

than control beam. Beams reinforced with welded metal mesh were given higher energy absorption than beams reinforced with expanded metal mesh or fibreglass mesh as see in Figure 8.
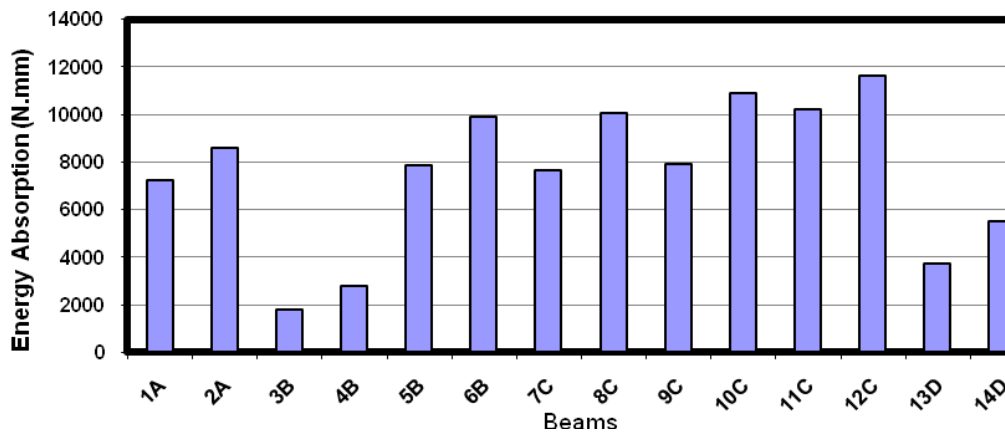

Figure 8. The Energy Absorption for all beams.

3.4   Behaviour of the Test Specimens

The behaviour of the test specimens in terms of load-deflection relationship, cracking behaviour, and mode of failure is discussed in the following sections.

3.4.1 Load-Deflection Relationship

The load-deflection curves of the control specimen (A1,A2), the specimens incorporating permanent ferrocement forms and reinforced with expanded steel mesh (designations B3, B4, B5,and B6), reinforced welded wire mesh (designations C7, C8, C9, C10, C11, and C12) and those reinforced with Fiberglas steel mesh(designations D13, D14) be divided into three stages as follows: Figures 9 to 12.

The load-deflection relationship for the control specimens was linear up to a load of 3000 N approximately after which the relation became non-linear. For this group of specimens, the transition from the second to the third stages, as explained before, was not distinct as shown in Figure 9. At failure, the mid-span deflection reached 26 mm, and 23.2 mm for specimens A1, A2 respectively. And the ultimate load was 6730 N, 8400 N for specimens A1, A2, respectively. A2 is better than A1 because max. Deflection is smaller than A1; the maximum load of A2 is greater than that of A1.

For group B (designations B3, B5) specimens reinforced with single layer of expanded wire mesh, the load-deflection relationship was almost linear up to load of about 780 N, 4150 N for specimens B3, B5 respectively when the deviation from the linear relation started. The maximum deflection reached 18.79 mm, 23.3 mm for specimens B3, B5 respectively.

When B4, B6 specimens reinforced with double layers of expanded wire mesh, the load-deflection relationship was almost linear up to load of about1000 N, 4000 N for specimens B4, B6 respectively when the deviation from the linear relation started as shown in Figure 10. At failure, the deflection reached 23 mm, 27.5 mm for beams B4, B6 respectively.

For group C (designations C7, C9 and C11) specimens reinforced with two layers of welded wire mesh, the load-deflection relationship was almost linear up to load of about 5000 N when the deviation from the linear relation started as shown in Figure 11. At failure, the deflection reached 20.77 mm, 20.9 mm, and 22.12 mm for beams C7, C9, and C11 respectively. When beams C8, C10 and C12) specimens reinforced with four layers of welded wire mesh, the load-deflection

relationship was almost linear up to load of about 5000 N. The maximum deflection was 24.5 mm, 23.59 mm, and 22.18 mm for beams C8, C10, and C12 respectively.

For group D (D13) specimen reinforced with single layer of fibreglass mesh, the load-deflection relationship was almost linear up to load of about 700 N when the deviation from the linear relation started as shown in Figure 12. At failure, the deflection reached 21.1 mm. For D14 specimen reinforced with double layers of fibreglass mesh, the load-deflection relationship was almost linear up to load of about 3000 N when the deviation from the linear relation started. The maximum deflection reached 20.75 mm.
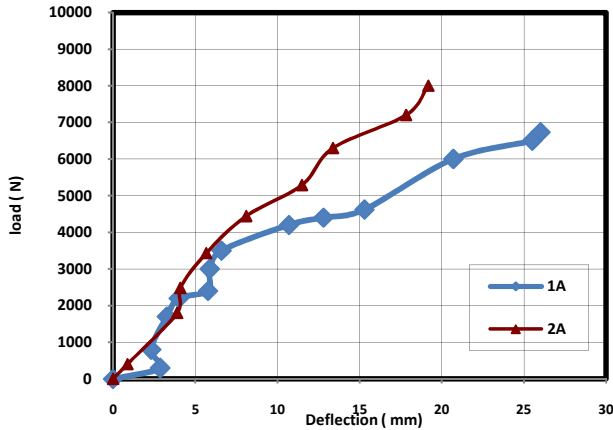

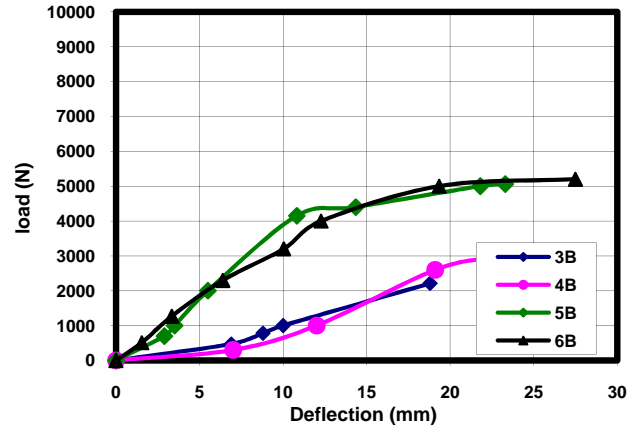Figure 9. load-Deflection Curves for group A
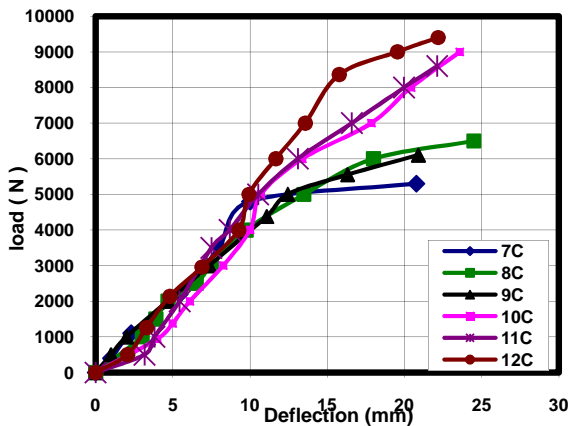

Figure 10. load-Deflection Curves for group B.

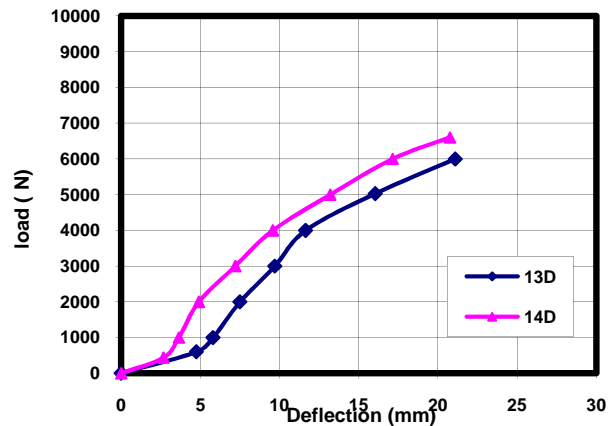
Figure 11. Load-deflection curves for group C

Figure 12. load-deflection curves for group D

3.4.2 Mortar Strain

Mortar strains were measured at four points at mid span of the test. Points 1, 2 were at 1 cm, 3 cm from top of beam respectively. Points 3, 4 were at 7 cm, 9 cm from top of beam respectively.

For Control A group specimens, the compressive strain at the gauge location increased with the increase of the applied load. The maximum compressive strain at this location reached about 1.2x10-4 strain at a load of 8400 N. The compressive strain at gauge location number 2 followed similar trend. However, the strain at this location was less than that at location number 1.While the tensile strains at locations number 3 and 4 increased with the increase of the applied load with the strain at location number 3 being less than that at location number 4. At failure, the tensile strain reading reached $8.2x10^{-5}$ strain at location number 4. as shown in Figure 13.

For group B (B3, B5) specimens reinforced with single layer of expanded wire mesh, the compressive strain at the gauge location (location no. 1) increased almost linearly up to load of 700 N when deviation from the linear relationship started. The maximum compressive strain at this location reached about $9.5x10^{-5}$ strain at a load of 5860 N. The compressive strain at gauge location number 2 followed similar trend. However, the strain at this location was less than that at location

number 1. The maximum compressive strain at this location reached about 8.6×10^{-5} strain at a load of 5860 N. The tensile strains at locations number 3 and 4 increased with the increase of the applied load with the strain at location number 3 being less than that at location number 4. At failure, the tensile strain reading reached 1.4×10^{-4} strain at location number 4 as shown in Figure 15.

For B4, B6 specimens reinforced with double layer of expanded wire mesh, the compressive strain at the gauge location (location no.1) increased almost linearly up to load of 1270 N when deviation from the linear relationship started. The maximum compressive strain at this location reached about 2.96×10^{-5} strain at a load of 6800 N. The compressive strain at gauge location number 2 followed similar trend. However, the strain at this location was less than that at location number 1. It is interesting to note that the tensile strains at locations number 3 and 4 increased with the increase of the applied load. The strain at location number 3 being less than that at location number 4.

At failure, the tensile strain reading reached 3.3×10^{-5} strain at location number 4. As shown in Figures 14 and 16.

For group C (designations C7, C9 and C11) specimens reinforced with two layers of welded wire mesh, the maximum compressive strain at this location reached about7.9×10^{-5}strain at a load of 6500 N. The compressive strain at gauge location number 2 followed similar trend. However, the strain at this location was less than that at location number 1. The tensile strains at locations number 3 and 4 increased with the increase of the applied load with the strain at location number 3 being less than that at location number 4.

At failure, the tensile strain reading reached 2.2×10^{-5} strain at location number 4 as shown in Figures 17, 19 and 21.

For group C (designations C8, C10andC12) specimens reinforced with four layers of welded wire mesh, the compressive strain at the gauge location (location no. 1) increased with the increase of the applied load. The maximum compressive strain at this location reached about 3.7×10^{-5} strain at a load of 11700 N. The compressive strain at gauge location number 2 followed similar trend. However, the strain at this location was less than that at location number 1. The maximum compressive strain at this location reached about 2.8×10^{-5} strain at a load of 11700 N. But the tensile strains at locations number 3 and 4 increased with the increase of the applied load with the strain at location number 3 being less than that at location number 4.

At failure, the tensile strain reading reached 3.2×10^{-5} strain at location number 4. Figures (18, 20 and 22) show load strain curves for beams in group C.

For group D (designations D13) specimens reinforced with single layer of fibreglass mesh, The maximum compressive strain at this location reached about 2.8×10^{-5} strain at a load of 6700 N. The compressive strain at gauge location number 2 followed similar trend. However, the strain at this location was less than that at location number 1. The maximum compressive strain at this location reached about1.7×10^{-5} strain at a load of 6700 N. Where the tensile strains at locations number 3 and 4 increased with the increase of the applied load with the strain at location number 3 being less than that at location number 4.At failure, the tensile strain reading reached 2.5×10^{-5} strain at location number 4.

For group D (designations D14) specimens reinforced with double layers of fibreglass mesh, The maximum compressive strain at this location reached about 2.2×10^{-5} strain at a load of 7200 N. The compressive strain at gauge location number 2 followed similar trend. However, the strain at this location was less than that at location number 1. The maximum compressive strain at this location reached about2.0×10^{-5} strain at a load of 7200 N. The tensile strains at locations number 3 and 4 increased with the increase of the applied load with the strain at location number 3 being less than that at location number 4.

At failure, the tensile strain reading reached 1.2×10^{-5} strain at location number 4. Figures 23 and 24 show load tensile strains for group D.
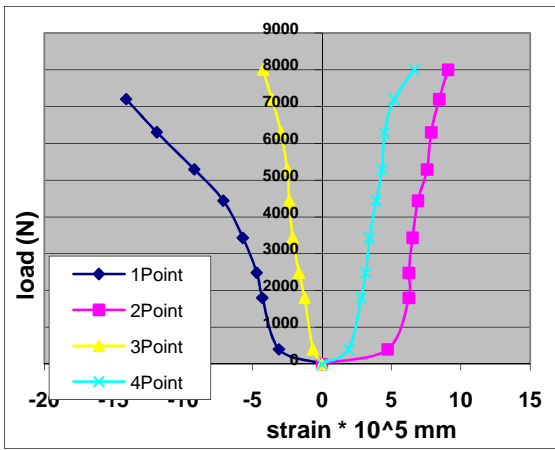
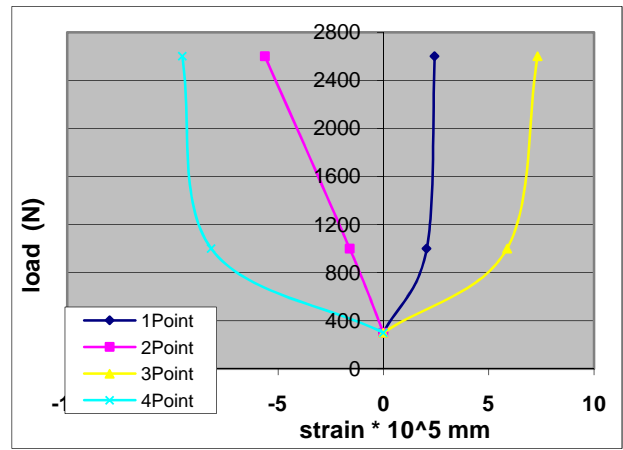Figure 13. Load - Strain Curves of A2

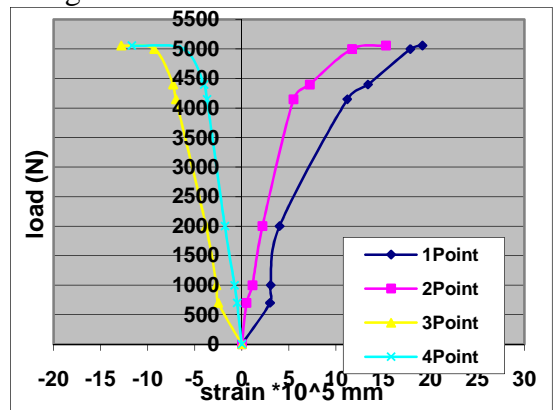
Figure 14. Load - Strain Curves of B4

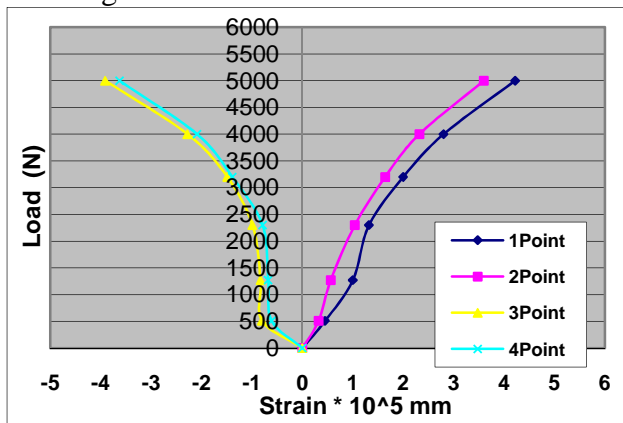Figure 15. Load - Strain Curves of B5

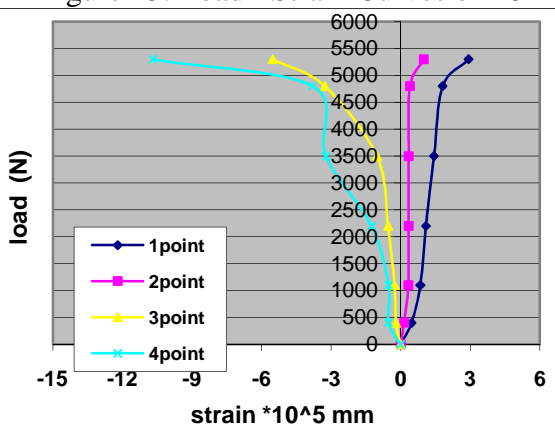Figure 16. Load - Strain Curves of B6

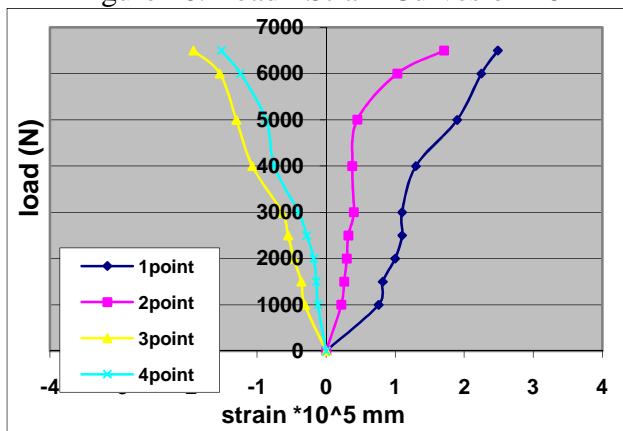Figure 17. Load - Strain Curves of C7
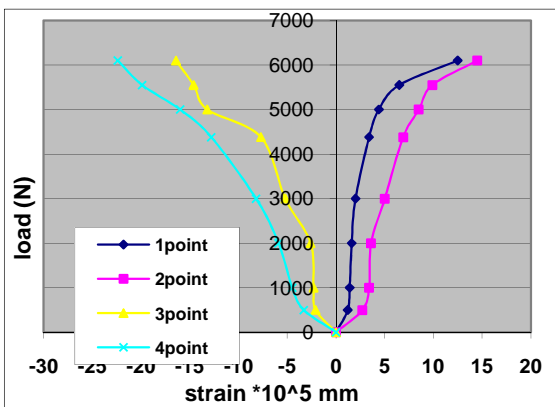

Figure 18. Load - Strain Curves of C8

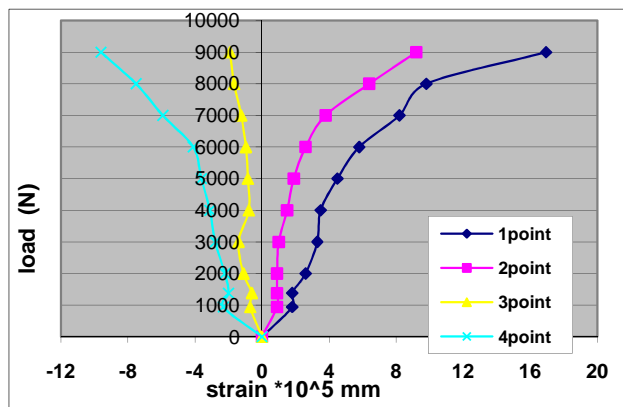Figure 19. Load - Strain Curves of C9

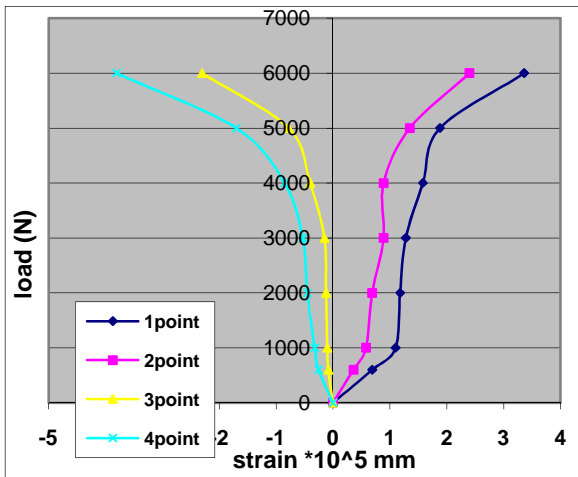Figure 20. Load - Strain Curves of C10
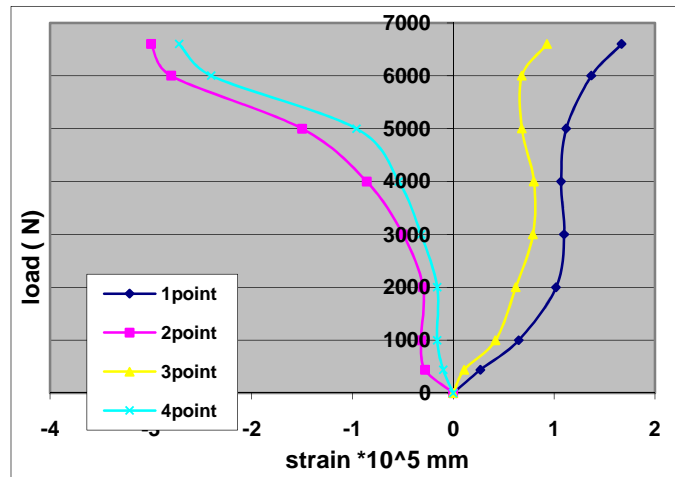
Figure 21. Load - Strain Curves of C11

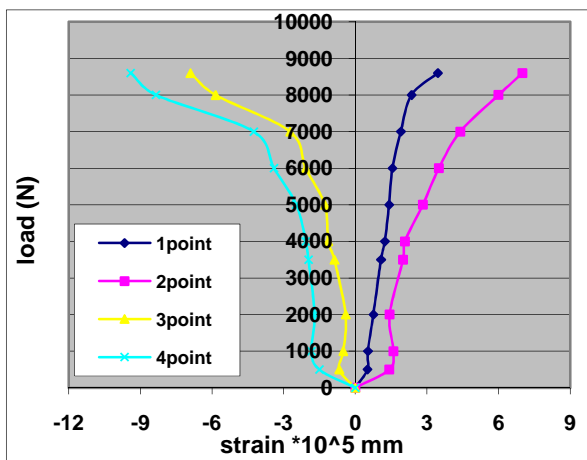Figure 22. Load - Strain Curves of C12

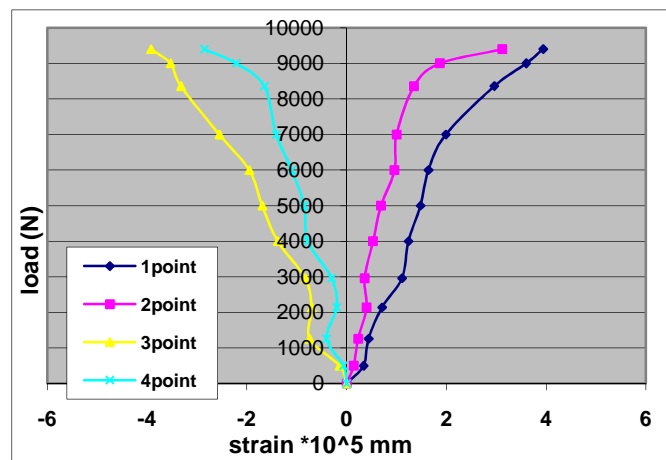Figure 23. Load - Strain Curves of D13

Figure 24. Load - Strain Curves of D14

3.5   Cracking Pattern and Mode of Failure
3.5.1 Control Specimen

Figure 25 shows the tensile crack, compressive crack and side views of crack patterns of all the tested beams. For designation A, flexural crack developed near the mid-span of the specimens of this designation at load of approximately 3000 N., for beam A1 and A2 and 4440 N. Upon increasing the load, the cracks propagated rapidly upwards and increased in number along the span. The length and width of the cracks increased with the increase of the applied load. Moreover, diagonal or inclined cracks developed at both ends of the specimen. Failure of the control specimens occurred due to the crushing of the concrete surface at load of 6730 N for A1 and 8400 N for A2 as shown in Figure 25.

3.5.2 Specimens incorporating Ferrocement Forms Reinforced with Expanded Steel mesh

For designation (B) beams B3, B4, B5 and B6, it is interesting to note that vertical flexural crack started to develop close to the centre of the span. As the load increased, more cracks started to develop in B5 and B6 and the crack at mid-span started to propagate vertically towards the top surface of the specimen, while there were almost no developed cracks in B3 and B4. The crack widths were much less than those of designation A. This could be attributed to the effect of No. of mesh layers in controlling the crack width.

Failure of this type of specimens occurred due to crushing of the concrete as shown in Figure 25.

### 3.5.3 Specimens incorporating Ferrocement Forms reinforced with welded Steel mesh

For designation (C) beams C7, C8, C9, C10, C11 and C12, it is interesting to note that vertical flexural crack started to develop close to the centre of the span. As the load increased, more cracks started to develop in C9, C10, C11 and C12 and the crack at mid-span started to propagate vertically towards the top surface of the specimen, while there were almost no developed cracks in C7 and C8. The crack widths were much less than those of designation A. This could be attributed to the effect of number of mesh layers in controlling the crack width.

The flexural crack developed near the mid-span of the specimens of this designation at load of approximately 5000 N., for beams C8, C9, C10 and C11 and 6000 N., for beams C12 and 4800 N., for beams C7. With the increase of the load, the cracks propagated vertically and new flexural cracks were developed rapidly.

As the specimens approached their failure load, the crack started to propagate wider. Failure of this type of specimens occurred due to crushing of the concrete. Spalling of the mortar cover at the bottom of some specimens occurred just after failure for C7and C8 as shown in Figure 26.

3.5.4 Specimens incorporating Ferrocement Forms reinforced with fibreglass Steel mesh

For designation (D) beams D13 and D14, it is interesting to note that vertical flexural crack for this type of specimens stared at mid-span and propagated vertically towards the top side of the beam and increased in number along the span. The rate of growth of crack propagation was less than that for the control specimen. Although the crack width was not measured in the test, the visual crack width was less than that of the control specimen. Failure of this type of specimens occurred due to flexural crack developed near the mid-span of the specimens of this designation at load of approximately1000 N, for beam D1 and 500 N for beam D2. Failure occurred due to the crushing of the concrete surface at load of 6000 N for A1and 6500 N for A2 as shown in Figure 26.
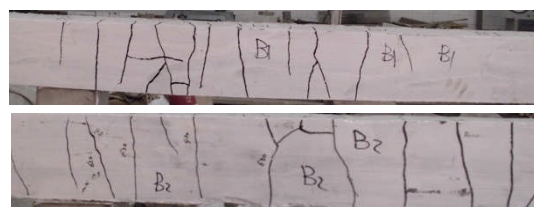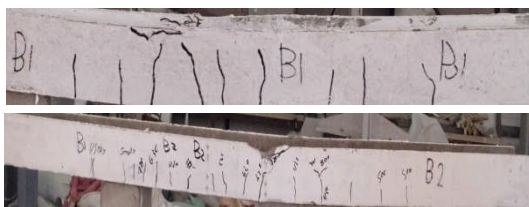
Crack Pattern from side of the beam   Crack Pattern from bottom of the beam

(a) Reinforcing Steel Bars for group A

Crack Pattern from side of the beam   Crack Pattern from bottom of the beam

(b) Expanded and Expanded with Steel Bars for group B.

Figure 25. The Cracking Pattern of Test Beams

Crack Pattern from side of the beam   Crack Pattern from bottom of the beam
(c) Welded and Welded with Steel Bars for group C.

Crack Pattern from side of the beam   Crack Pattern from bottom of the beam
(d) Fiberglas mesh with Steel Bars for group D
Figure 26. The Cracking Pattern of Test Beams.

3.6   Effect of the Test Parameters

The effect of the test parameter is investigated from the experimental results of the test specimens and is discussed in the following sections. The effects of these parameters were studied on the structural responses of the test beams in terms of first crack load, service load, and failure load, mode of failure, ductility ratio, and energy absorption.

The load-deflection relationship for the control specimens was linear up to a load of approximately 3000 N approximately, when the first crack was observed, after which the relation became nonlinearly. Beyond load of about 6730 N the mid-span deflection increased with much higher rate indicating yielding of the steel reinforcement. At failure, the mid-span deflection reached 26 mm.

3.6.1 Effect of the Existence of Synthetic Fibres in the Mortar Mix

The effect of the existence of the synthetic fibres in the mix of the ferrocement mortar on the behaviour of the test specimens is studied by comparing the results of the same specimens containing the fibres in the mix with the corresponding ones without the fibres for series A. and for all groups with other.

The behaviour of the specimens without synthetic fibres was considered as the base for this comparison. The existence of the synthetic fibres in the mortar mix resulted in an increase in the first crack load, serviceability load, ultimate load, and energy absorption. However, it resulted in a decrease in the ductility ratio. Figures 27 and 28 show the comparison between the load deflection curves for test specimens.

The existence of the synthetic fibres resulted in retarding the occurrence of the first crack and better crack distribution in the ferrocement U-shaped permanent forms. This led to a higher stiffness of the test specimen and consequently less deflection at the corresponding load levels as shown in Figure 27. The figures show that the specimens with fibre had a higher deflection at failure as a result of the attained higher ultimate load. However, the ratio of the deflection at ultimate load to that at the first cracking load was lower for the specimens with fibres in comparison to those without fibres, which led to the observed reduction of the ductility ratio as defined in this research.

3.6.2 Effect of the type of the mesh inside the U Shape Beam

The effect of reinforcing steel mesh type is studied by comparing the results of groups reinforced with expanded wire mesh to that reinforced with welded steel mesh and fibreglass mesh. Figure 28 shows the load deflection curves for groups B, D compared to group C.

The behaviour of expanded wire mesh group was considered as the base for comparison for both single and double layers. While samples reinforced with welded wire mesh achieved higher first crack load, ultimate load, serviceability load and energy absorption with respect to steel bars and the number of steel mesh

It is worth mentioning that the ductility of beams reinforced with expanded wire mesh is higher than that of beams reinforced with welded wire mesh. This is expected since the specimens reinforced with expanded steel mesh had slightly higher volume fraction, 0.0075 as compared with 0.003, however, the proof stress for the expanded steel mesh, 199 N/mm^2 was much lower than that for the welded wire mesh, 400 N/mm^2.

3.6.3 Effect of the Number of Reinforcing Steel Mesh Layers

The effect of the number of reinforcing steel mesh layers is investigated by comparing the results of groups reinforced with single and double layers for both steel mesh types investigated in this research. Doubling the steel mesh layers at the bottom of the specimens resulted in a higher first crack load, serviceability load, ultimate load, and energy absorption. However, the maximum deflection at ultimate load decreased as a result of increasing the specimen's stiffness also the ductility ratio decreased due to the increase of the volume fraction.

The enhancement in mechanical properties due to increasing the number of steel mesh layers for welded wire mesh was much higher than that of expanded wire mesh for the first crack load, ultimate load, and serviceability load and energy absorption. However, the enhancement in reduction in the ductility ratio was almost the same for both types of steel mesh.
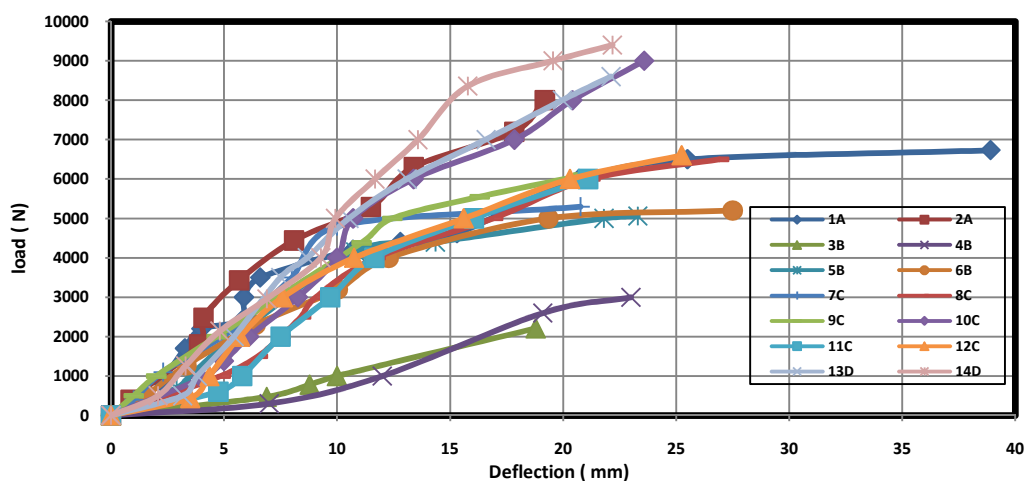

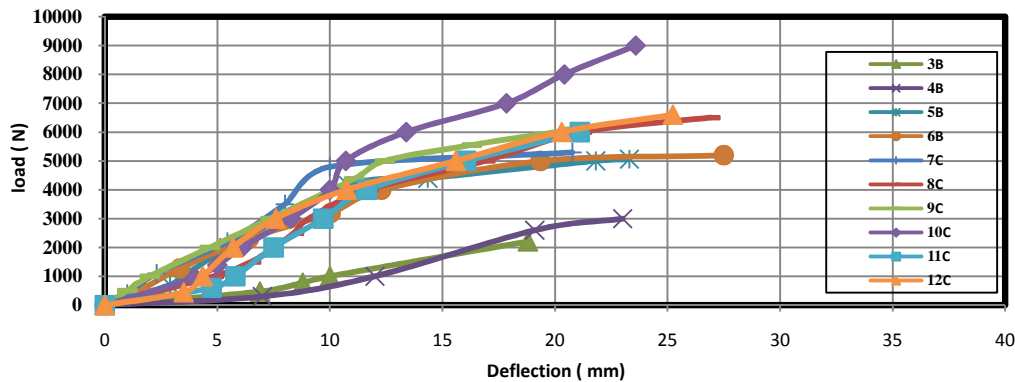**Figure 27. Comparing the Results of all Beams.**

Figure 28. Comparing the Results of Groups B, C.

4. **Conclusions**

The results also demonstrated that the presence of fibres in the mix improved the beam's overall performance. Within the scope, parameters considered in this research and based on the test results and observations of the experimental investigation; the following conclusions and recommendations could be drawn as follows:

1. Using welded steel mesh gave the highest results compared to all tested beams.
2. Employing polypropylene fibres in mortar mix increase in the first crack load, serviceability load, ultimate load, and energy absorption, higher stiffness However, it resulted in a decrease in the ductility ratio, less deflection at the corresponding load levels.
3. Welded wire mesh achieved higher first crack load, serviceability load, ultimate load and energy absorption in comparison to reinforce with expanded and fibreglass mesh.
4. Using (two - four) layers of welded metal mesh in reinforcing ferrocement beams, improve the energy absorption obtained than that when using skeletal steel bars.
5. Using U-shaped welded mesh with mild steel bars in reinforcing ferrocement beams gave higher energy absorption than that of using mild steel bars only. However the U-shaped showed less ductility ratio.
6. Using two mild steel bars with one layer expanded metal mesh improve ductility ratio and energy absorption compared to that using two-layer expanded metal mesh only.
7. Increasing the number of the steel mesh layers in the ferrocement forms increases the first crack load, service load, ultimate load, and energy absorption decreases.
8. Using welded wire mesh reinforcement decreased the ductility ratio compared to that reinforced with fibreglass mesh and expanded steel mesh.
9. The percentage of reduction ductility ratio depends on the type and number of steel mesh layers in the ferrocement forms.

References:

[1] American Concrete Institute (2009) ACI Committee 549-1R-93, *"Guide for the Design, Construction, and Repair of Ferrocement,"* Manual of Concrete Practice, Farmington Hill, Michigan, USA. 27 pages.
[2] Antoine E. Naaman, and Surendra P. Shah, *"Tensile Tests of Ferrocement,"* ACI Journal, September 1971, pp.693-698.
[3] Hala Mohamed Refat Abd ElMohimen (2005) *"Structural Behaviour of Ribbed Ferrocement Plate",* B.SC. Thesis submitted to Menoufia University, Egypt.
[4] Arshdeep Singh Channi (July 2009) *"Effect of Percentage of Reinforcement on Beams Retrofitted with Ferrocement Jacketing",* Thapar University Patiala-147004.
[5] E. H. Fahmy, Y. B. Shaheen, and M. N. Abou Zeid (2004) *"Development of Ferrocement Panels for Floor and Wall Construction",* 5th Structural Specialty Conference of the Canadian Society for Civil Engineering, June 2-5.

[6] Mansur and P. Paramasivam, *"Ferrocement Short Columns Under Axial and Eccentric Compression,"* ACI Structural Journal Title, No. 87-S52, September- October, 1990, pp. 523-529

[7] Ramesht and J. G. Vickridge, *"FAOFERRS- A Computer Program for the Analysis of Ferrocement in Flexure,"* Journal of Ferrocement, Vol. 26, No. 01, January, 1996, pp. 21- 31.

[8] Singh , E. W. Bennettand N. A. Fakhri, *"Influence of Reinforcement on Fatigue of Ferrocement,"* The InterNational Journal of Cement Composites and Lightweight Concrete, August, 1988, Vol. 8, No. 03, pp.151-164.

[9] Yara Mahmoud El-Sayd El-Sakhawy (2000) *"Structural Behaviour of Ferrocement Roof Elements",* B.Sc. Thesis submitted to Menoufia University, Egypt.

[10] Anshu Tomar *"Retrofitting of Shear Deficient R.C. Beams Using Ferrocement Laminates",* deemed university Patiala- (June 2006)147004.

[11] Abdel Tawab, Alaa (2006) *"Development of Permanent Formwork for Beams Using Ferrocement Laminates",* Ph.D. thesis submitted to Menoufia University, Egypt.

[12] Abdul Kadir, Mohd. Razali, and Jaafar, Mohd. Saleh Hj. (1993) *"Ferrocement in Situ Permanent Formwork"*, Journal of Ferrocement, Vol. 23, No. 2, pp. 125-133.

[13] Abdul Kadir, Mohamed Razali, Abdul Samad, Abdul Aziz, Che Muda, Zakaria, and Ali, Abang Abdullah Abang, *"Flexural Behaviour of Composite Beam with ferrocement Permanent Formwork"*, Journal of Ferrocement, (1997) Vol. 27, pp. 209 - 214.

[14] El-Halfawy, E. (2003) *"Flexural Behavior of Ferrocement Deck Bridges",* M.Sc. thesis, Faculty of Engineering, Menoufia University, Shebin El-Kom, Egypt.

[15] Fahmy, E.H., and Shaheen, Y.B. (1991) *"Strengthening and Repairing of Reinforced Concrete Tanks"*, Fourth Arab Structural Engineering Conference, pp.18-21

[16] Fahmy, E.H., Shaheen, Y.B.I., and El-Dessouki, W. M. (1995) *"Application of Ferrocement for Construction of Radial Gates,"* Journal of Ferrocement, Vol. 25, No. 02, April, pp.115-121.

[17] Fahmy, E.H., Shaheen, Y.B.I., and Korany, Y.S., January (1997) *"Repairing Reinforced Concrete Beams by Ferrocement"*, Journal of Ferrocement, Vol. 27, No. 1, pp. 19-32.

[18] Fahmy, E.H., Shaheen, Y.B.I., and Korany, Y.S., April (1999) "*Repairing Reinforced Concrete Columns Using Ferrocement Laminates",* Journal of Ferrocement, Vol. 29, No. 2, pp. 115-124.

[19] Mays, G.C. and Barnes, R.A. (1995) *"Ferrocement Permanent Formwork as Protection to Reinforced Concrete"*, Journal of ferrocement, Vol. 25, No.4, pp. 331-345.

[20] Naaman, Antoine E., and Shsh, Surendra P., *"Tensile Tests of Ferrocement",* ACI Journal, September 1971, pp. 693 – 698.

[21] Rao, P.K. and Rao, V.J. (1987) "*Development and application of Composite Precast Ferrocement and Concrete Roofing/Flooring System.*" Proceedings of the First International Conference on Structural Science and Engineering, India.

[22] Rosenthal, I. and Bljuger, F. (1985) "*Bending Behaviour of Ferrocement – Reinforced Concrete Composite".* Journal of ferrocement, Vol. 15, No.1, pp. 15-24.

[23] R. N. Swamy and M.I. Abboud, *"Application of Ferrocement Concept to Low Cost Lightweight Concrete Sandwich Panels"*, Journal of ferrocement, Vol. 18, No. 3, July 1988.

[24] Shorouk Taha Abd EL-Ghani Ayoub (2005) *"Flexural Behaviour of High Strength Concrete Beams Reinforced with Advanced Composite Materials",* M.Sc. Structural Engineering, Minufia University.

[25] Ashwaq M. Hafiz (2012)*" Structural Behaviour of Ferrocement channels Beams"* M.Sc. thesis submitted to Menoufia University, Egypt.

[26] Doha El M. Kandil (2013)*" Impact Resistance of Reinforced Ferrocement Concrete Plates":* M.Sc. thesis submitted to Menoufia University, Egypt.

[27] E.C.P. 203/2007, 2007, Egyptian Code of Practice: Design and Construction for Reinforced Concrete Structures, Research Centre for Houses Building and Physical Planning, Cairo, Egypt.

[28] E.S.S. 1109/2008, 2008, Egyptian Standard Specification for Aggregates, Egypt.

[29] E.S.S. 4756-1/2009, 2009, Egyptian Standard Specification for Ordinary Portland Cement, Egypt.

[30] ASTM C 494-03, 2003, American Society for Testing and Materials: Chemical Admixtures, Philadelphia, USA.

[31] E.S.S. 262 /2011, 2011, Egyptian Standard Specification for Steel Bars, Egypt.